

Experimental Evidence of Space Charge Driven Emittance Coupling in High Intensity Linear Accelerators

L. Groening, I. Hofmann, W. Barth, W. Bayer, G. Clemente, L. Dahl, P. Forck, P. Gerhard, M. S. Kaiser, M. Maier, S. Mickat, T. Milosic, and S. Yaramyshev

GSI Helmholtzzentrum für Schwerionenforschung GmbH, Planckstrasse 1, D-64291 Darmstadt, Germany

D. Uriot

CEA IRFU, Service des Accélérateurs, de Cryogénie et de Magnétisme, F-91191 Gif-sur-Yvette, France

(Received 19 August 2009; published 25 November 2009)

In high intensity linacs emittance exchange driven by space charge coupling may lead to the well-known “equipartitioning” phenomenon if the stop band at $\sigma_{\parallel} = \sigma_{\perp}$ is crossed at sufficiently slow rate. This Letter is the first experimental evidence of this phenomenon in a high intensity linear accelerator, here the UNILAC at GSI. Measurements of emittances at the entrance and exit of one drift tube linac tank comprising 15 lattice cells are taken for a set of transverse and longitudinal tunes. The onset of exchange on the stop band of previously derived “stability charts” confirms theoretical predictions. The measured transverse emittance growth also compares well with results from the beam dynamics simulation codes DYNAMION and TRACEWIN.

DOI: 10.1103/PhysRevLett.103.224801

PACS numbers: 29.27.Bd, 41.75.-i, 41.85.-p

The Universal Linear Accelerator (UNILAC) serves as injector for the heavy ion accelerator facility at GSI [1]. It can accelerate all ion species from protons to uranium to an energy of up to 11.4 MeV/u. In order to cover the wide range of ion masses, the rf field strengths and the magnetic quadrupole field strengths can be adjusted depending on which ion needs to be provided. For the ion $^{40}\text{Ar}^{10+}$ the full range of stable transverse zero current phase advances of up to 180° can be set. This operational flexibility requires enhanced availability of beam diagnostics devices compared with linacs that need to provide beams of one ion species only. These two features, along with the stable and optimized operation of the machine and efforts to minimize initial mismatch, have provided the foundation for recent successful campaigns for beam dynamics code benchmarking [2] and for the verification of the 90° space charge resonance [3,4]. They are equally crucial for the present experimental study of the space charge induced 4th-order coupling resonance $2\sigma_{\parallel} - 2\sigma_{\perp} = 0$ known as “resonant equipartitioning” or emittance coupling driven by initial anisotropy [5–8]. The process is collective and related to the so-called collisionless electrostatic Harris instabilities in anisotropic uniform plasmas or beams (see Ref. [9]). Although never demonstrated directly in linac experiments, avoiding this resonance has become a widely accepted design constraint for most high intensity linacs [10–12]. In some other facilities fast crossing is tolerated [13]. On the other hand, taking advantage of this emittance coupling by deliberately tuning to the resonance condition was proposed for the design of radio frequency quadrupoles [14]. In a related direction the proposal of *a priori* “equipartitioned linacs” to avoid undesirable emittance exchange issues was made in Refs. [15,16].

As the longitudinal emittance of the UNILAC is almost 10 times larger than the transverse, the theoretically predicted emittance coupling should result in a visible increase of the transverse emittance in high current operation even over a relatively short distance. The experiment was carried out using the first tank of the UNILAC’s Alvarez-type drift tube linac (DTL) as shown schematically in Fig. 1. Along this tank ions are accelerated from 1.4 to 3.6 MeV/u using an rf frequency of 108 MHz. Longitudinal beam focusing is achieved by operating -30° from rf crest, while transverse focusing uses a quadrupolar *F-D-D-F* lattice. The tank has 63 rf gaps and each of the 62 drift tubes houses one quadrupole such that the DTL comprises 15 complete lattice cells. A dedicated matching section in front of the DTL is used for rms matched injection into its periodic lattice. Behind the DTL an additional slit-grid setup for transverse emittance measurement and a beam transformer for beam transmission control were used. For the 7.1 mA $^{40}\text{Ar}^{10+}$ beam the transverse zero current phase advance $\sigma_{\perp,0}$ was varied from 35° to 80° , keeping the longitudinal zero current phase advance constant at 43° . Accordingly, the depressed

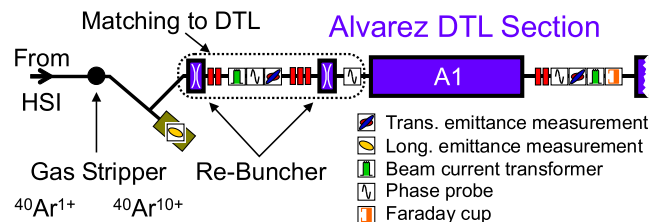


FIG. 1 (color online). Schematic setup of the experiments as from Ref. [3] (not to scale).

TABLE I. Phase advances at the entrance to the DTL in the case of zero current and depressed tune ratios for 7.1 mA of $^{40}\text{Ar}^{10+}$ of an rms equivalent beam with a Kapchinsky-Vladimirsky distribution.

$\sigma_{\perp,o}$ (deg)	$\sigma_{\perp}/\sigma_{\perp,o}$	$\sigma_{\parallel}/\sigma_{\perp}$
34.8	0.76	1.55
44.3	0.80	1.14
49.9	0.83	0.98
55.0	0.84	0.87
60.0	0.85	0.79
70.0	0.88	0.65
79.9	0.89	0.56

tune ratio $\sigma_{\parallel}/\sigma_{\perp}$ was varied from 0.6 to 1.5. The procedure of setting up the beam up to injection into the DTL including the verification of proper rms matching for each value of $\sigma_{\perp,o}$ is described in detail in [17]. Using the mismatch definition of [18] the residual longitudinal mismatch was estimated as 0.5 and the horizontal and vertical one as 0.1, respectively. These values are sufficiently low to avoid transverse rms emittance growth by mismatch, which was checked by simulation. Beam emittance measurements in front of the DTL revealed normalized rms emittances of 0.15/0.22 mm mrad (horizontal/vertical). The normalized longitudinal rms emittance was found to be 1.8 mm mrad. Table I shows the resulting transverse tune depressions as well as the depressed tune ratio for the applied values of $\sigma_{\perp,o}$.

Using these rms emittance values the corresponding Hofmann stability chart [8] can be created, which has the given ratio of longitudinal to transverse rms emittances as free parameter (in Fig. 2 a ratio of 10 is used based on the average transverse emittances).

The intensity of the blue shaded area in Fig. 2 is proportional to the amount of expected emittance exchange per unit distance. Note that the main peak is associated—in the limit of low intensity—with the 4th-order coupling resonance $2\sigma_{\parallel} - 2\sigma_{\perp} = 0$. Two spurious peaks at $3\sigma_{\parallel} - \sigma_{\perp} = 0$, respectively $2\sigma_{\parallel} - \sigma_{\perp} = 0$, have negligible effect [8]. It should be noted that much stronger transverse tune depression (below 0.5) removes the isolated stop bands, and emittance coupling results for all tune ratios, with the exception of very small tune ratios (0.2, . . . , 0.1), where the beam becomes increasingly equipartitioned anyway (it is exactly equipartitioned for a tune ratio approaching the inverse of the emittance ratio [10]).

The beam's particle distribution in the six-dimensional phase space at the DTL entrance has been reconstructed as described in [2] based on the emittance measurements in front of the DTL. This distribution has been used to calculate the beam's path within the stability chart with the simulation code DYNAMION [19]. Figure 2 shows the paths for various $\sigma_{\perp,o}$ values. It is noted that the tune trajectory

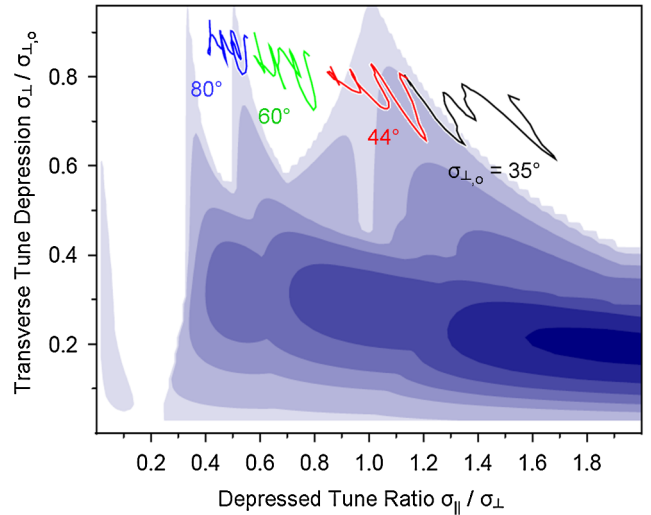


FIG. 2 (color online). Example of Hofmann stability chart for emittance ratio 10 and simulated paths of the depressed tunes for transverse zero current phase advances $\sigma_{\perp,o}$ of 35°, 44°, 60°, and 80°.

for $\sigma_{\perp,o} = 44^\circ$ completely overlaps with the main stop band, which is fully crossed.

After setting the DTL quadrupoles to the desired phase advance $\sigma_{\perp,o}$ horizontal and vertical phase space distributions have been measured at the DTL exit as shown in Fig. 3. From the distributions normalized rms emittances have been extracted. Figure 4 plots the mean of horizontal and vertical emittance, i.e., $(\epsilon_{\text{rms},x} + \epsilon_{\text{rms},y})/2$ as a function of the depressed tune ratio $\eta = \sigma_{\parallel}/\sigma_{\perp}$ at the entrance to the DTL. For $\eta \leq 0.8$ a constant value of the transverse rms emittance has been measured within the accuracy of the measurement, which is estimated to be 5%. As η approaches 1.0 from below, a considerable transverse emittance growth by about 20% with respect to the values measured for $\eta \leq 0.8$ is observed. For $\eta \rightarrow 1.5$ the measured emittance shows a further increase not explained by the stability chart, while simulation indicates a slight in-

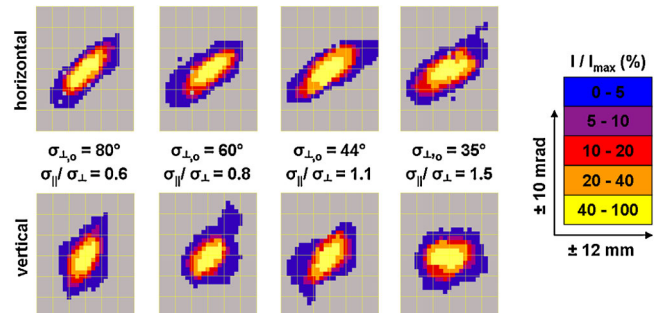


FIG. 3 (color online). Phase space distributions measured at the DTL exit for zero current phase advances $\sigma_{\perp,o}$ of 35°, 44°, 60°, and 80°. Upper panels: horizontal; lower panels: vertical. The scale is ± 12 mm and ± 10 mrad. Fractional intensities refer to the phase space element including the highest intensity.

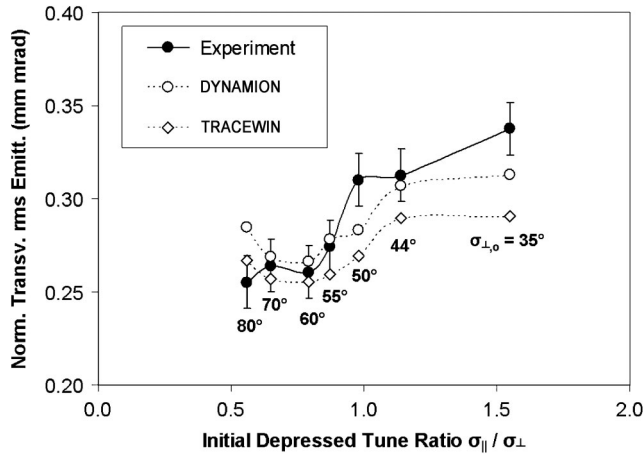


FIG. 4. Mean of horizontal and vertical rms emittance at the DTL exit as a function of the initial ratio of depressed longitudinal and transverse tune $\eta = \sigma_{\parallel}/\sigma_{\perp}$.

crease. This experimental result is in good agreement with beam dynamics simulations performed with two different codes, i.e., DYNAMION and TRACEWIN [20]. Experimental data and simulations agree well on the overall dependence of the emittance on the tune ratio as well as on the absolute values. They also reflect the presence of the main stop band within the stability chart (Fig. 2).

For this reasons we attribute the observed transverse emittance growth at $\sigma_{\parallel} \approx \sigma_{\perp}$ to resonant emittance exchange from the longitudinal plane to the transverse plane. Accordingly, the longitudinal rms emittance should shrink for the resonance case. The limited space behind the DTL tank did not allow for measurements of the longitudinal phase space distribution. Additionally, for intense argon beams the UNILAC's total longitudinal emittance at the DTL entrance exceeds the area of the rf bucket. The unavoidable rf-bucket overflow causes longitudinal rms emittance growth during acceleration. This growth is expected to mitigate the longitudinal emittance shrinking driven by emittance exchange. As the sum of emittances is expected to be constant [8] the relative longitudinal decrease from this source cannot exceed 10%, which would be hard to measure in any case. Therefore, we depend on indirect evidence by considering two circumstances. (1) Confidence in the results of the applied simulation codes is sufficiently high in order to justify the use of longitudinal distributions from simulations instead of those from measurements. (2) Any reduction in rms emittance should manifest itself as increased phase space density inside the initial distribution core as long as this core is small with respect to the rf-bucket area.

We have therefore evaluated the particle current confined within the ellipse having the size of the rms emittance at the DTL entrance. This evaluation has been done for each plane separately. To obtain a meaningful value for the current within a given ellipse area, the ellipse parameters β and α as well as the ellipse center must be chosen such that

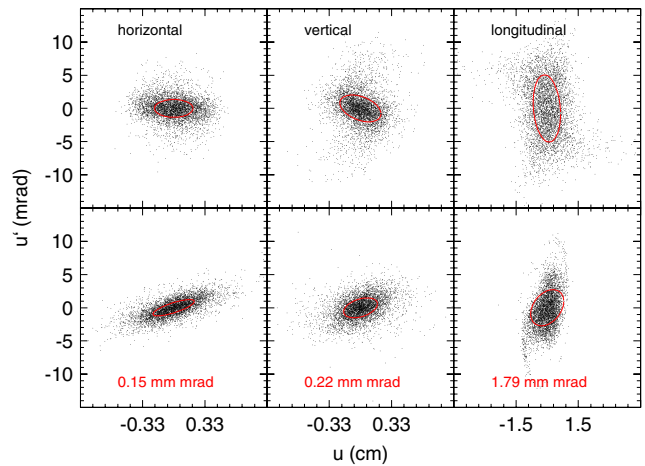


FIG. 5 (color online). Phase space distributions (u, u' referring to the horizontal/left, vertical/center, and longitudinal/right coordinate) corresponding to the $\sigma_{\perp,o} = 60^\circ$ case from simulations with the DYNAMION code. Top: DTL entrance; bottom: DTL exit.

the confined number of particles is at maximum. Figure 5 shows particle distributions from DYNAMION simulations at the entrance and at the exit of the DTL. Additionally, the ellipses confining the area corresponding to the rms ellipse at the DTL entrance are plotted for each plane [in gray

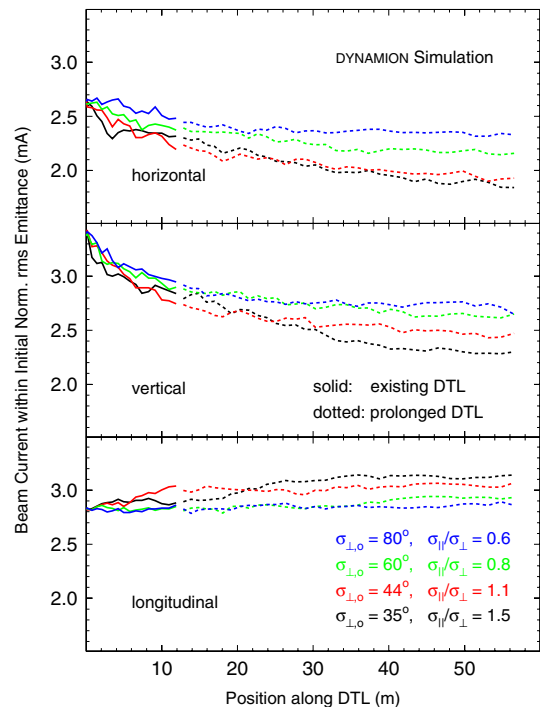


FIG. 6 (color online). Beam current within the initial rms emittance as a function of position using the DYNAMION code. Solid lines correspond to the DTL used for the measurements, while dotted lines indicate results corresponding to a virtually prolonged DTL.

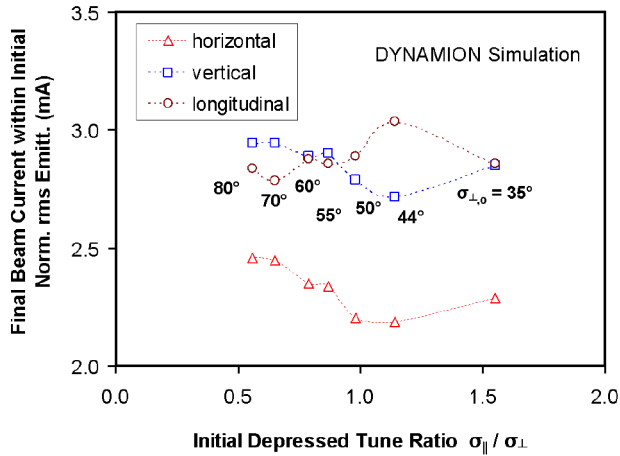


FIG. 7 (color online). Simulated beam currents within the initial rms emittance at the DTL exit as a function of the initial ratio of depressed longitudinal and transverse tune $\sigma_{\parallel}/\sigma_{\perp}$.

(red)]. The amount of particles within these ellipses is a measure for the phase space density within the distribution core.

The beam current within the initial rms emittance was evaluated for each plane as a function of the position along the DTL beam line. Figure 6 plots the results for four different tune ratios. In the two transverse planes the core density decreases along the DTL. The slope of the decrease increases with the depressed tune ratio. The transverse decrease is accompanied by the increase of the longitudinal core density during acceleration as expected from the beam's path within the stability chart. This observation is a strong evidence for emittance exchange from the longitudinal plane to the transverse planes and it agrees very well with the measurements of transverse emittances. Core densities at the end of the DTL are plotted in Fig. 7 as a function of the tune ratio η at the DTL entrance. The final transverse core density generally decreases as η approaches 1.0, where it shows a minimum. The longitudinal density shows the complementary behavior, i.e., a maximum for $\sigma_{\parallel} \approx \sigma_{\perp}$. In the simulations the DTL was prolonged virtually in order to increase the emittance exchange effect as shown by the dotted lines in Fig. 6. Comparison of the longitudinal curves for the cases of $\eta = 1.5$ and for $\eta = 1.1$ indicates that the density increase for $\eta = 1.5$ sets in at a later time with respect to the increase for $\eta = 1.1$. This delay follows directly from the paths within the stability chart showing that the beam related to $\eta = 1.5$ enters the resonance later with respect to the beam related to $\eta = 1.1$.

In summary, we conclude that the experimental observations jointly with the results from simulations provide evidence for the existence of resonant emittance exchange along a high intensity linac. Good agreement was found with the predictions from the theoretical stability charts, which are thus experimentally benchmarked as valid design tools.

-
- [1] W. Barth *et al.*, in *Proceedings of the XXII Linac Conference, Lübeck, 2004*, edited by V.R. W. Schaa (DESY, Hamburg, 2004), p. 246.
 - [2] L. Groening *et al.*, *Phys. Rev. ST Accel. Beams* **11**, 094201 (2008).
 - [3] L. Groening *et al.*, *Phys. Rev. Lett.* **102**, 234801 (2009).
 - [4] D. Jeon *et al.*, *Phys. Rev. ST Accel. Beams* **12**, 054204 (2009).
 - [5] R. A. Jameson, in *Proceedings of the Third Workshop on Advanced Accelerator Concepts, Port Jefferson, NY, 1992*, AIP Conf. Proc. No. 279 (AIP, New York, 1992), p. 969.
 - [6] I. Hofmann and O. Boine-Frankenheim, *Phys. Rev. Lett.* **87**, 034802 (2001).
 - [7] I. Hofmann *et al.*, in *Proceedings of the European Particle Accelerator Conference, Paris, 2002*, edited by J.L. Laclare (CERN, Geneva, 2002), p. 74.
 - [8] I. Hofmann *et al.*, *Phys. Rev. ST Accel. Beams* **6**, 024202 (2003).
 - [9] E. A. Startsev *et al.* *Phys. Rev. ST Accel. Beams* **8**, 124201 (2005).
 - [10] T.P. Wangler, *Rf Linear Accelerators* (Wiley-VCH, Weinheim, 2008), 2nd ed., p. 319.
 - [11] A.M. Lombardi *et al.*, in *Proceedings of the 42nd ICFA Advanced Beam Dynamics Workshop on High-Intensity and High-Brightness Hadron Beams, Nashville, TN, 2008*, edited by C. Horak (SNS, Oak Ridge, TN, 2008), p. 238.
 - [12] P.N. Ostroumov, *New J. Phys.* **8**, 281 (2006).
 - [13] J. Stovall *et al.*, in *Proceedings of the Particle Accelerator Conference, Chicago, 2001*, edited by P. Lucas (IEEE, New York, 2001), p. 446.
 - [14] R. A. Jameson, ORNL Technical Report No. ORNL/TM-2007/001, 2007.
 - [15] M. Reiser and N. Brown, *Phys. Rev. Lett.* **74**, 1111 (1995).
 - [16] M. Reiser, *Theory and Design of Charged Particle Beams* (Wiley-VCH, Weinheim, 2008), 2nd ed., p. 611.
 - [17] L. Groening *et al.*, in *Proceedings of the 10th International Computational Accelerator Physics Conference, San Francisco, 2009*, edited by J. Chew (unpublished).
 - [18] see Ref. [10], p. 222.
 - [19] S. Yaramyshev *et al.*, *Nucl. Instrum. Methods Phys. Res., Sect. A* **558**, 90 (2006).
 - [20] <http://irfu.cea.fr/Sacm/logiciels/index.php>.